Characteristics of pellets with immobilized activated sludge and its performance in increasing nitrification in sequencing batch reactors at low temperatures

Wenjie Dong[1], Guang Lu[2], Li Yan[3,*], Zhenjia Zhang[4], Yalei Zhang[1]

1. College of Environmental Science and Engineering, Tongji University, Shanghai 200092, China
2. Wenzhou Housing and Urban–Rural Development Committee, Wenzhou 325000, China
3. Wenzhou Public Utilities Investment Group Co. Ltd., Wenzhou 325000, China
4. Environmental Science and Engineering, Shanghai Jiaotong University, Shanghai 200240, China

ARTICLE INFO

ABSTRACT

Immobilized pellets obtained by means of entrapping activated sludge in waterborne polyurethane were successfully adapted in ammonium (NH_4^+–N) synthetic wastewater. Its physicochemical characteristics were determined using scanning electron microscope, pyrosequencing, and microelectrodes, and its influence on the nitrification process in sequencing batch reactors (SBRs) at low temperatures was evaluated. A large number of rod-shaped bacteria were observed on the surface of the immobilized pellet, in which *Rudaea* spp. (Xanthomonadaceae family) was an important bacterial component (23.44% of the total bacteria). The oxygen uptake rate of immobilized pellets reached 240.83 ± 15.59 mg O_2/(L·hr), and the oxygen was primarily consumed by the bacteria on the pellet surfaces (0–600 μm). The dosing of the pellets (30 mL/L) into an SBR significantly improved the nitrification efficiency at low temperatures of 7–11 °C, achieving an average NH_4^+–N removal of 84.09%, which is higher than the removal of 67.46% observed for the control group.

© 2015 The Research Center for Eco-Environmental Sciences, Chinese Academy of Sciences. Published by Elsevier B.V.

Introduction

Ammonium (NH_4^+–N) in wastewater is derived from the enzymatic breakdown of urea, proteins, and other nitrogen-containing materials. It is widely accepted that NH_4^+–N is toxic to several fish species in an aqueous solution even at low concentrations (0.1 mg/L) (Eshchar et al., 2006) and can be transformed into nitrite (NO_2^-–N) and nitrate (NO_3^-–N) in drinking water, which can confer risks to human health, such as infant methemoglobinemia and gastric cancer (Bruning-Fann and Kaneene, 1993; Ward et al., 2005). Thus, NH_4^+–N must be removed from wastewater before being discharged into a water body.

As an efficient and economical technology for NH_4^+–N removal, biological treatment is widely applied in wastewater treatment plants (WWTPs), but low temperatures (<15 °C) would sharply reduce the activity of microorganisms, such as nitrobacteria, leading to poor NH_4^+–N removal (Fdz-Polanco et al., 1994; Sudarno et al., 2011). Therefore, feasible methods to enhance NH_4^+–N removal at low temperatures are desired.

* *Corresponding author.* E-mail: Vangji@126.com (Li Yan).

Traditional practices have been carried out to improve NH_4^+–N removal by adjusting operating parameters, such as sludge load, return sludge, aeration rate, and hydraulic retention time (HRT) (Salem et al., 2003; Wu et al., 2007), but it is still difficult to achieve high treatment efficiency or reduced operation costs in biological systems at low temperatures. Another alternative method is bio-augmentation to enhance the nitrification process in a biological system *via* psychrotrophs (Ben et al., 2009; Chevalier et al., 2000; Huang et al., 2015), granular sludge (de Kreuk et al., 2005) or bacterial immobilization (Isaka et al., 2007, 2008). Due to the slow growth of microbes at low temperatures, it is hard to maintain responsible psychrotrophs as the predominant species or takes a long time to form stable granular sludge in biological systems. Therefore, a simpler and more effective method is still desired.

The immobilization technique entraps microorganisms in the interior of a porous material and has several advantages (Hashimoto and Sumino, 1998; Sumino et al., 1992; Qiao et al., 2010), such as easy preparation, a long biomass retention time and resistance to shock load, which are especially beneficial for the slow growth of nitrifying activated sludge. Thus, immobilization might be an effective method for enhancing NH_4^+–N removal at low temperatures. Isaka et al. (2007) reported using nitrifying bacteria entrapped in a polyethylene glycol gel carrier to obtain stable nitrification rates at 10 °C for high concentrations of NH_4^+–N in landfill leachates. Dong et al. (2011) also used entrapment of activated sludge pellets in waterborne polyurethane for the continuous treatment of micro-polluted water and achieved an NH_4^+–N removal rate of over 80%. Unfortunately, oxygen profiles and oxygen uptake rate have not been well characterized in these pellets. Recently, microelectrode measurements have been known as the most reliable techniques to directly measure the microenvironment and activity of microorganisms in their habitats with a high spatial and temporal resolution (Xiao et al., 2013; Hou et al., 2014; Ali et al., 2015). Furthermore, little work has been done to evaluate the nitrification activity for domestic sewage using immobilized pellets at low temperatures.

Hence, the aim of this work is to reveal the physicochemical characteristics of pellets obtained from entrapped activated sludge in waterborne polyurethane by means of scanning electron microscopy (SEM), pyrosequencing and microelectrode measurements. Furthermore, immobilized pellets were added to a sequencing batch reactor (SBR) to evaluate the performance in increasing nitrification for the treatment of artificial wastewater at low temperatures.

1. Materials and methods

1.1. Immobilized pellets

Elastic gel immobilized pellets (cubes with 3-mm-long sides, black, unscented, density of 1.02 g/cm^3) were obtained by means of entrapping activated sludge (20 g/L) in waterborne polyurethane, as described in previous reports (Dong et al., 2011, 2012). Artificial wastewater was used for acclimation of immobilized pellets in order to activate and produce more nitrobacterium. The compositions contained (per liter) NH_4Cl, 306.0 mg; $NaHCO_3$, 936.0 mg; KCl, 18.9 mg; NaCl, 41.0 mg;

$Na_2HPO_4 \cdot 12H_2O$, 92.6 mg; $CaCl_2 \cdot 2H_2O$, 18.9 mg and $MgSO_4 \cdot 2H_2O$, 67.2 mg. The acclimation experiments were conducted in an up-flow inner circulation aerated reactor (Dong et al., 2011). The working volumes of the reactor and pellets were 18 L and 1.8 L, respectively (packing ratio of 10%). To ensure sufficient dissolved oxygen (DO: 3–4 mg/L) and mixing, air was supplied from the bottom of the reactor using a stone air diffuser. The initial pH was in the range of 7.2–7.4, and the temperature was 18 °C in the reactor during the acclimatization period. The HRT was controlled at 4 hr by adjusting the feed flow rate. About 15 days, the acclimatization was deemed to finish when the average NH_4^+–N concentrations in the effluents were less than 5 mg/L.

1.2. Morphological observation by SEM

The surface and cross-sectional morphological characteristics of the immobilized pellets were examined by SEM (S-3000N SEM, Hitachi, Japan). Pellets sampled from the up-flow inner circulation aerated reactor on day 0 and day 20 represent un-acclimated pellets and acclimated pellets, respectively. The collected samples were rinsed with 0.1 mol/L phosphate buffer three times, fixed with 2.5% glutaraldehyde solution for 12 hr at 5 °C, dehydrated through a graded ethanol series up to 100%, and dried with a critical point dryer (K850, Quorum Technologies Ltd., UK). These samples were cut in half with a sterile scalpel for observing cross-sectional images, and the preparative surfaces and cross sections of the immobilized pellets were sputtered with gold for SEM observations.

1.3. Microbial community analysis by pyrosequencing

Microbial communities in un-acclimated and acclimated immobilized pellets were analyzed by pyrosequencing. Sample pretreatment and DNA extraction were performed according to a report by Isaka et al. (2012). Sequences of the 16S rRNA gene including the variable V3 region were amplified with two primers: tP2 (5′-acgtacatATTACCGCGGCTGCT-3′) and tP3 (5′-acgtacatCCTACGGGAGGCAGCAG-3′) (Zhang et al., 2011). Polymerase chain reaction (PCR) amplification was performed using a thermal cycler PCR system (PCR Sprint, Thermo electron, UK). The PCR products were evaluated by 1.2% (W/V) agarose gel electrophoresis and purified with a Gel/PCR DNA Fragment Extraction Kit (Geneaid, UKAS). Amplicon libraries were prepared using a mixture of three independent PCR products for each sample. The concentration of the PCR amplicons was measured using a Fluoroskan Ascent with a Quant-iT PicoGreen dsDNA reagent (Invitrogen, USA). Samples for 454 pyrosequences were sent to the Chinese National Human Genome Center in Shanghai, which performed amplicon pyrosequencing using a standard Roche 454/GS-FLX Titanium (McKenna et al., 2008).

Sequences obtained from pyrosequencing reads were processed to remove short sequences with lengths less than 100 nucleotides, primer mismatches, or average quality scores lower than 25. The sequences were verified in Ribosomal Database Project II (RDP Release 10) using Chimera Check (http://rdp.cme.msu.edu/index.jsp), and all chimeric sequences were discarded. The taxonomic identities of sequences were assigned using the Classifier program of the RDP-II at a confidence level of 80% (Zhong et al., 2014).

1.4. Oxygen uptake rate measurement

The oxygen uptake rate (OUR) is defined as the amount of oxygen consumed per unit time and per unit volume of pellets. A micro-respiration system (Unisense, Denmark) was used for measuring the rate of decrease of the DO concentration. This high-precision test system mainly includes an oxygen micro-respiration sensor, micro-respiration chambers, a micro-respiration rack, a picoammeter, *etc.* The detailed process of the OUR measurement is as follows. First, the micro-respiration sensor was calibrated at two points: the zero value (achieved by an anoxic alkaline ascorbic acid solution) and the saturation value (obtained by bubbling with air). Second, feed water and 0.50 mL of pellets (the actual volumes measured by drainage) were added into a micro-respiration chamber. Third, the chambers were placed on a submerged rack in a temperature-regulated water bath. Finally, the sensor was put into the chamber, and the signals of the DO concentration were recorded by micOx software.

Specific oxygen uptake rate (SOUR) of activated sludge in SBRs during the aeration phase is determined by mixed liquor suspended solids (MLSS) and the rate of decrease of the DO concentration (d[DO]/dt) of the mixed liquor in the micro-respiration chamber, which is calculated using Eq. (1):

$$SOUR = \frac{1}{MLSS} \frac{d[DO]}{dt} \tag{1}$$

1.5. Microsensor profiles

Oxygen profiles are obtained using a Clark-type microelectrode with a tip diameter of 10–20 μm (Unisense, Denmark). The microelectrode was calibrated as the micro-respiration system mentioned above. During the calibration procedure, the temperature and salinity in the solutions should be the same as that of the feed water for accurate measurement. Due to the minute tip size, excellent response time and insignificant stirring sensitivity, the oxygen microelectrode could provide reliable and fast measurements with a high spatial resolution. In this test, 0.25-mm acupuncture needles were used for fixing pellets into a homemade foam box. The fixed pellets were immersed in the oxygen-saturated water, and they were not allowed to touch the box surface. The entire foam box was installed at the Unisense lab stand LS18. The precise test position of the microelectrode was controlled by a motorized micromanipulator (model MM-33, Unisense, Denmark).

1.6. SBR apparatus and operating conditions

Two SBRs with a working volume of 100 L (length 78.5 cm × width 40.5 cm × height 39 cm) were applied, in which SBR-1 and SBR-2 were used for the experimental group and blank group, respectively. Artificial wastewater was used for SBR experiments. The compositions contained the following (per liter): NH_4Cl, 126 mg; $NaHCO_3$, 386 mg; KCl, 7.8 mg; NaCl, 16.9 mg; $Na_2HPO_4 \cdot 12H_2O$, 38.2 mg; $CaCl_2 \cdot 2H_2O$, 7.8 mg; $MgSO_4 \cdot 2H_2O$, 27.7 mg and glucose, 270 mg. To discharge activated sludge and prevent immobilized pellet loss, a hole with mesh was made at the bottom of the SBRs. Air was introduced through stone air diffusers to maintain the DO in a range of 2 to 3 mg/L during the aeration phase. The SBRs were inoculated with activated sludge from the aerobic tank of a WWTP in Wenzhou, China. Sludge concentrations in the reactors were maintained at 4000–4600 mg/L. The operating cycle of the SBRs comprised four phases lasting 1 hr each: the first phase involved feeding in stirred conditions, the second phase was aeration, the third phase was settling, and finally, treated water discharge was released in the fourth phase. To determine whether the nitrification would be enhanced in SBR-1, acclimated immobilized pellets were added after the removal rate of chemical oxygen demand (R-COD_{Cr}) and NH_4^+–N remained constant at low temperatures. This experiment was performed over 180 cycles at temperatures of 7 to 11 °C in water.

NH_4^+–N, NO_2^-–N, NO_3^-–N, total nitrogen (TN), COD_{Cr}, sludge volume (SV_{30}) and MLSS were determined according to the standard methods (CEPB, 2002).

2. Results and discussion

2.1. Characteristics of immobilized pellets

2.1.1. SEM observation
Fig. 1 shows bacteria spatial distributions on un-acclimated pellets and acclimated pellets. It was observed that un-acclimated pellets contained an embedding matrix with a large pore space framework (Fig. 1a). These pores were necessary for substance transportation into and out of pellets. In this study, both the peripheral surface and the cross-sectional surface were compared between un-acclimated and acclimated pellets. In Fig. 1a and c, few spherical, rod-shaped and irregular particles were observed on the two surfaces of un-acclimated pellets. In contrast, there were large amounts of rod-shaped microbes covering the pellet surfaces. In the picture of the cross-sectional surface (Fig. 1e), these rod-shaped microbes were primarily distributed on the outer layer, whereas microbes on the inner layer were very limited (Fig. 1f). These microbes were tightly arranged and formed a dense biological film on the pellet surfaces. The thickness of the biological film was approximately 80–120 μm. Thus, the decreasing concentrations of NH_4^+–N during acclimation periods should be ascribed to the formation of a biological film on the pellet surfaces.

2.1.2. Determination of bacterial species in immobilized pellets
In the experiment of 454 pyrosequencing, the total number of effective sequences that passed quality control was 1796 and 2820 in un-acclimated and acclimated pellets, respectively. Table 1 summarizes the bacterial compositions at the phylum and class levels. At the phylum level, Proteobacteria was the predominant microorganism in both the un-acclimated and acclimated pellets, accounting for 38.04% and 49.43% of the total bacteria, respectively. At the class level, Anaerolineae, classified in the Chloroflexi phylum, was the dominant microorganism in the un-acclimated pellets (18.22%), but it was very limited in the acclimated pellets (<1%). In contrast, Gammaproteobacteria, which belongs to the Proteobacteria phylum, was the dominant microorganism in the acclimated pellets (26.24%), and its abundance was much higher than the percentage in the un-acclimated pellets (4.51%). In addition, due to the limited detection techniques, several bacterial
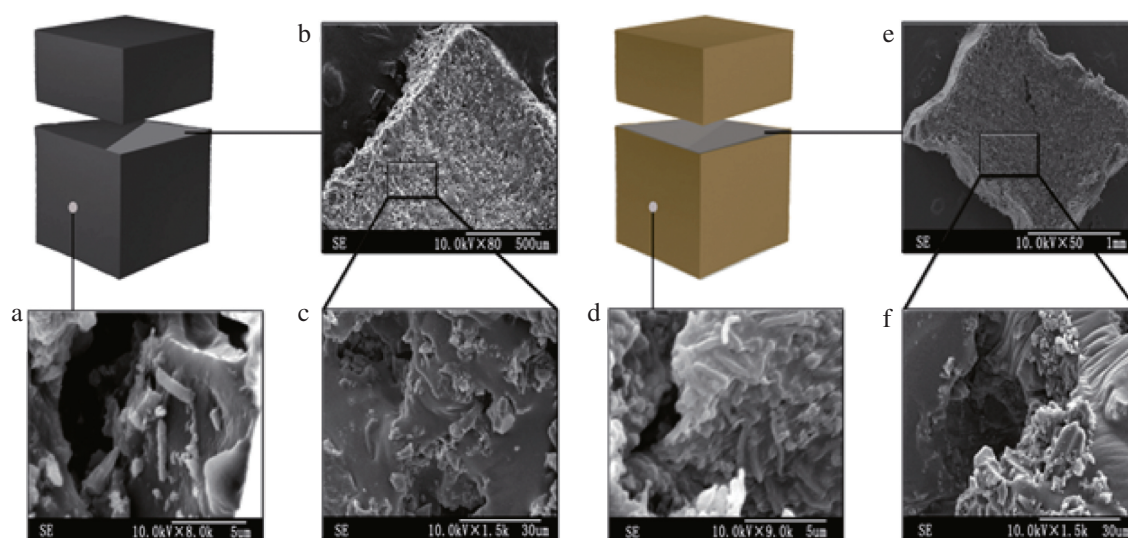
Fig. 1 – Scanning electron microscopy (SEM) images of the immobilized pellets. (a) Peripheral surface of the un-acclimated pellets. (×8000) bar length: 5 μm; (b, c) cross-sectional image of un-acclimated pellets. (×1500) bar length: 30 μm and (×80) bar length: 500 μm, respectively; (d) peripheral surface of the acclimated pellets. (×9000) bar length: 5 μm; (e, f) cross-sectional image of the acclimated pellets. (×1500) bar length: 30 μm and (×50) bar length: 1000 μm, respectively.

sequences could not be classified into any phylum, accounting for 23.56% and 17.41% of the total bacteria in the un-acclimated and acclimated pellets, respectively.

The community structures between un-acclimated pellets and acclimated pellets were further classified at the family level. As shown in Fig. 2, the bacteria of the un-acclimated pellets and the acclimated pellets could be classified into 48 and 43 families, respectively. Several bacterial species related to the nitrification process, including *Xanthomonadaceae*, *Chitinophagaceae*, *Nitrospiraceae*, *Comamonadaceae*, *Cystobacteraceae*, *Nitrosomonadaceae* and *Planctomycetaceae*, were observed in the acclimated pellets (Fitzgerald et al., 2015; Gomez-Alvarez et al., 2013; Khardenavis et al., 2007), whereas these bacteria were sparse in the un-acclimated pellets. Additionally, at the genus

level, a bacterial species named *Rudaea* spp. was the dominant microorganism in the acclimated pellets, accounting for 23.44% of the total bacteria. *Rudaea* spp. was first classified as an aerobic, rod-shaped bacterium in the Xanthomonadaceae family in 2009 (Weon et al., 2009). To our best knowledge, this microbe has not been identified as being to the nitrification process; however, it may play an important role based on the results of this study. Thus, a further identification experiment about the nitrification function of this single species is worth to be carried out.

2.1.3. Respiratory intensity and oxygen distribution in immobilized pellets

The activity of bacteria can be reflected by the respiratory intensities of immobilized pellets. Fig. 3 shows the DO

Table 1 – Percentages of sequences identified to different phylogenies.			
Phyla	Class	Un-acclimated pellets	Acclimated pellets
Actinobacteria	Actinobacteria	4.68%	4.01%
Bacteroidetes	Sphingobacteria	1.50%	7.94%
Proteobacteria	Deltaproteobacteria	4.12%	5.67%
	Betaproteobacteria	21.50%	10.78%
	Alphaproteobacteria	7.91%	6.74%
	Gammaproteobacteria	4.51%	26.24%
Nitrospira	Nitrospira	3.84%	5.53%
Gemmatimonadetes	Gemmatimonadetes	–	3.05%
Acidobacteria	Acidobacteria_Gp4	–	1.70%
	Acidobacteria_Gp6	1.06%	–
	Acidobacteria_Gp16	–	1.35%
Firmicutes	Clostridia	2.73%	–
	Bacilli	–	3.16%
Planctomycetes	Planctomycetacia	–	2.59%
Chloroflexi	Anaerolineae	18.22%	–
	Minor class [*]	6.35%	3.83%
Unclassified	Unclassified	23.56%	17.41%

[*] Rare class with less than 1% abundance were grouped as "Minor class".
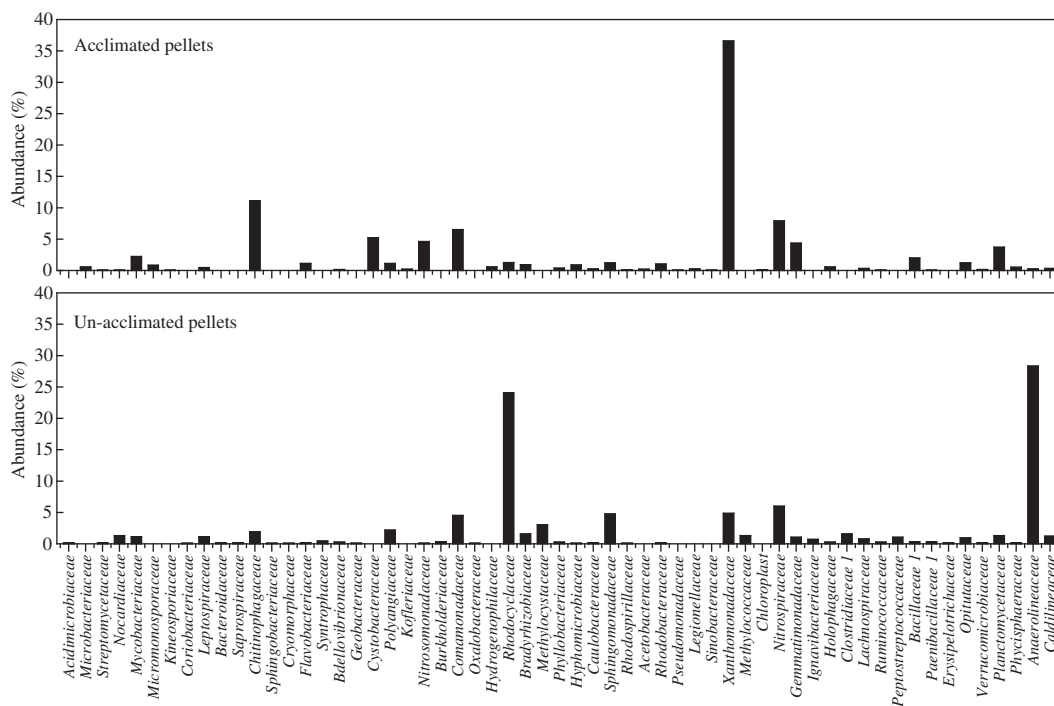
Fig. 2 – Relative phylotype frequency at the family level.

concentration changes for un-acclimated pellets (line a) and acclimated pellets (line b). DO (initial concentration of 8.5 mg/L) in the micro-respiration chamber was exhausted after an inoculation of 15 hr, with an average OUR of 5.53 mg O_2/(L·hr) of un-acclimated pellets. In contrast, the DO can be absolutely consumed within 1 min, and the average OUR of acclimated pellets reached 239.63 mg O_2/(L·hr), which was 43-fold higher than that of un-acclimated pellets (Fig. 3, line b). These data indicate that the microorganisms on the surface of acclimated pellets have high aerobic activity, consistent with rapid oxygen consumption during the nitrification process.

The distribution of oxygen in immobilized pellets can reflect the exact positions at which the oxygen consumption process

occurs. Fig. 4 shows the differences in the oxygen distributions between the un-acclimated pellets and the acclimated pellets. The distribution of oxygen on un-acclimated pellets resulted in a V-shaped graph, of which the minimum DO concentration occurred at the center of the pellets and its value remained above 7.2 mg/L. The average descent gradient of oxygen from the surface to the center was only 0.002 mg O_2/(L·μm). These data demonstrate that the efficiency of oxygen transfer in the embedding medium was very high, whereas the oxygen consumption by microorganisms was very limited in the un-acclimated pellets. In contrast, the oxygen on acclimated pellets showed a U-shaped distribution. In Fig. 4, the distribution of oxygen shows a drastic decline from the surface to a depth of 300 μm, and to a depth of 600 μm, the oxygen concentration
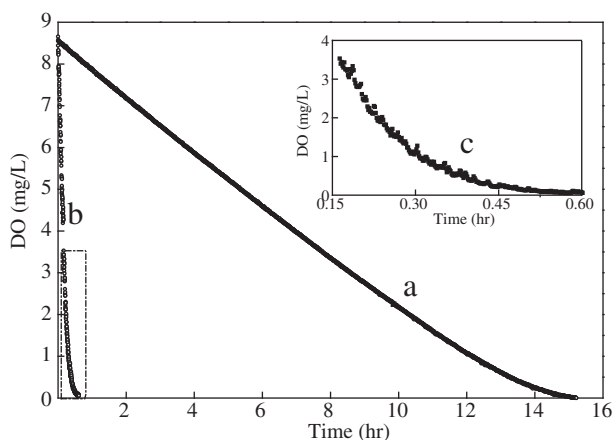

Fig. 3 – Respiratory intensity of the immobilized pellets. Line a: un-acclimated pellets; Line b: acclimated pellets; Line c: partial enlarged sectional view of Line b.
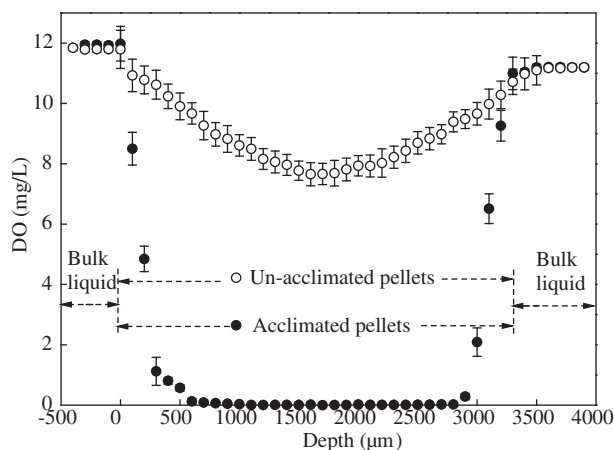

Fig. 4 – Oxygen microprofiles of immobilized pellets. (Depth zero is the pellet surface, mean ± SE, n = 3).

was close to 0 mg/L. The average oxygen descent gradient of 0–300 μm reached 0.035 mg O_2/(L·μm) in the acclimated pellets, which was 17-fold higher than that of the un-acclimated pellets. The results suggest that the consumption of oxygen was mainly focused on the surface of acclimated pellets, which was consistent with the microorganism distributions and community compositions.

2.1.4. Nitrification performance of immobilized pellets

Fig. 5 shows the changes in the OUR values and the NH_4^+–N removal rate during acclimation periods. During initial periods (0–10 days after inoculation), the values of OUR were very low (only in the range of 4.11 to 26.62 mg O_2/(L·μm)), consistent with low efficiencies (0.02%–28.57%) of NH_4^+–N removal. These data indicate that the biological films on the surface of immobilized pellets are not well formed 10 days after inoculation. In contrast, the values of OUR and NH_4^+–N removal efficiency sharply increased after 15 days of inoculation, achieving an OUR of 240.83 ± 15.59 mg O_2/(L·μm) and an NH_4^+–N removal efficiency of 90%. Similarly, the values of OUR and NH_4^+–N removal efficiency remained relatively constant during the latter periods (15–30 days). This indicates that the biological film is fully formed on the pellet surfaces on the 15th day after inoculation. Throughout the whole operational period, there was a significant positive correlation ($R^2 = 0.976$) between OUR and the NH_4^+–N removal efficiency, indicating that the oxygen consumption mainly resulted from nitrification.

2.2. SBR experiments

2.2.1. Effects of immobilized pellets on NH_4^+–N removal

The enhancement in the nitrification performance due to the addition of acclimated pellets was evaluated, including the operation in SBR-1 and the control group (only using single activated sludge) in SBR-2. Fig. 6 presents the differences in NH_4^+–N removal between SBR-1 with immobilized pellets and the control group in SBR-2. The effluent NH_4^+–N concentrations in

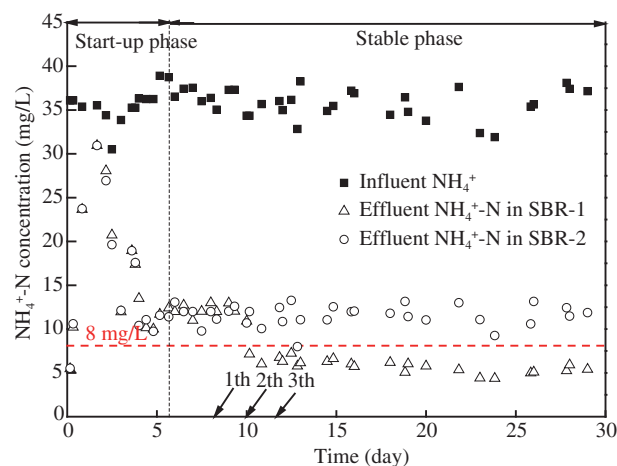**Fig. 6 – Variations of NH_4^+–N concentrations in the sequencing batch reactors (SBRs).**

the two reactors increased during the initial phase (1–3 days) because the inoculated activated sludge was not readily available for the intermittent operation mode in the SBR systems at low temperatures. With the two reactors operating until the 6th–8th day, the NH_4^+–N and COD_{Cr} concentrations in the effluents remained relatively stable, indicating that the activated sludge had adapted to the operation mode. Thus, the immobilized pellets were first added into SBR-1 on the 8th day after activated sludge inoculation. However, there were no significant differences in the effluent NH_4^+–N concentrations between SBR-1 and SBR-2, which is due to the low quality of the pellet additions (10 mL/L). Therefore, more acclimated pellets were added on the 10th and 12th day such that the total addition of acclimated pellets was 30 mL/L. As a result, the effluent NH_4^+–N concentrations in SBR-1 began to decline, and the mean value was 5.67 mg/L, which was below the discharge standard (8 mg/L) of WWTPs in China at low temperatures (< 12 °C). In contrast, the average NH_4^+–
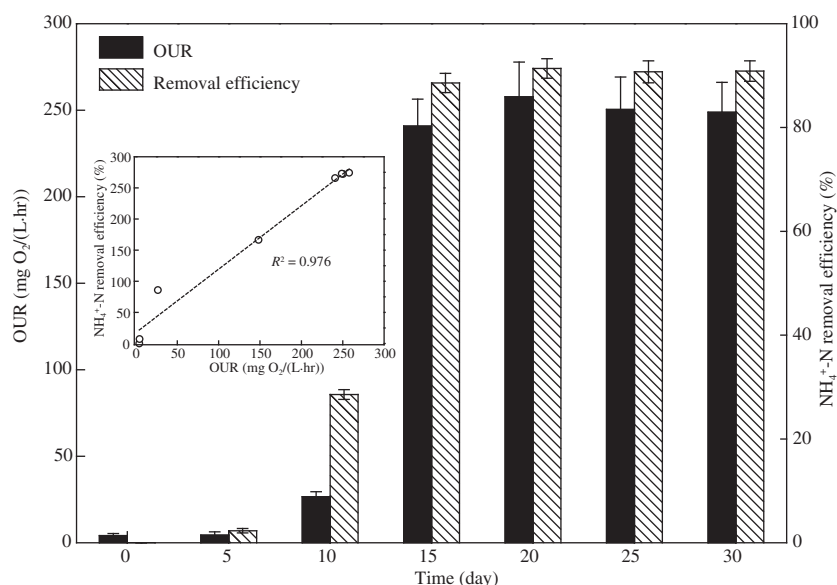
Fig. 5 – Variations of oxygen uptake rate (OUR) and NH_4^+–N removal efficiency. (mean ± SE, n = 3).

N concentration in the effluents from SBR-2 reached 11.59 mg/L, which was obviously higher than that of SBR-1 and did not meet the discharge standard of WWTPs in China. With the help of immobilized pellets, the average removal efficiency of NH_4^+–N in SBR increased to 84.09%, whereas without immobilized pellets, NH_4^+–N removal was only 67.46%. These data show that the addition of immobilized pellets can enhance nitrification performance in SBRs and ensure that the effluent NH_4^+–N concentrations are below the discharge standards at low temperatures (<12 °C). It is worth noting that the immobilized pellets were acclimated at 18 °C for the purpose of quick acclimation, but the temperature in the SBR was lower (7–11 °C), which may cause a short-term activity of nitrobacteria in the pellets. Fortunately, the results of NH_4^+–N removal efficiency in SBR-1 show that the change of temperature does not reduce the nitrification of the pellets significantly, which indicated that the pellets have a strong resistance to lower temperatures.

2.2.2. Analysis of nitrogen-containing compounds in the SBRs

To evaluate the effects on the concentrations of nitrogen-containing compounds due to the addition of immobilized pellets into the SBR, NO_2^-–N and NO_3^-–N and TN were analyzed in the effluents during the stable phase. The average NO_2^-–N concentration of the effluents in SBR-1 and SBR-2 were 1.99 and 1.91 mg/L, respectively. The average effluent NO_3^-–N concentration in SBR-1 (3.58 mg/L) was slightly higher than that in SBR-2 (3.12 mg/L). Therefore, the effluent NO_2^-–N and NO_3^-–N concentrations were not significantly different in the two SBRs. The average TN concentration of the effluents was 12.01 mg/L in SBR-1, which was lower than 16.96 mg/L in SBR-2. Thus, not only did the addition of immobilized pellets enhance the nitrification performance in the SBR, but it also helped with the removal of TN. The removal of TN is completed by nitrification and denitrification processes and/or the synthesis of biomass. In this present study, the enhancement of nitrification might supply more substrates for the process of denitrification at low temperatures.

2.2.3. Analysis of activated sludge in the SBRs

To exclude the effects of the differences in activated sludge on the nitrification process, the characteristics of active sludge in the two SBRs were evaluated, including SV_{30}, MLSS, SOUR and R-COD_{Cr}. As shown in Table 2, the characteristics of activated sludge were very similar between the two SBRs. This indicates that the enhancement of nitrification performance mainly results from the addition of acclimated pellets rather than

from changes in activated sludge characteristics. In addition, although the R-COD_{Cr} in the two SBRs approached 90%, the SOUR values were consistently lower than 5.00 mg O_2/(g MLSS·hr) in the two SBRs, which was much lower than the values reported in other studies (Chen et al., 2001; Gikas and Livingston, 1998), indicating that low temperatures had a serious effect on the sludge activity. In view of the average NH_4^+–N concentration, the effluents from SBR-2 did not meet the discharge standard of WWTPs in China, and it could be speculated that nitrifying bacteria in the SBRs were limited by the low temperature. Thus, at low temperatures, the addition of acclimated pellets into the SBR was necessary to achieve effective nitrification.

3. Conclusions

The SEM images revealed that large amounts of rod-shaped bacteria covered the surfaces of immobilized pellets, and *Rudaea* spp. (Xanthomonadaceae family) was important bacterial species (23.44% of the total bacteria). The mean OUR value of immobilized pellets reached 240.83 ± 15.59 mg O_2/(L·hr); the oxygen was consumed by the bacteria on the pellet surfaces (0–600 μm). The SBR experiments demonstrated that the addition of immobilized pellets (30 mL/L) significantly improved nitrification efficiency at low temperatures of 7 to 11 °C, removing 84.09% of the total NH_4^+–N from wastewater.

Acknowledgments

R E F E R E N C E S

Ali, M.M., Oshiki, M., Rathnayake, L., Ishii, S., Satoh, H., Okabe, S., 2015. Rapid and successful start-up of anammox process by immobilizing the minimal quantity of biomass in PVA-SA gel beads. Water Res. 49 (79), 147–157.

Ben, Y., Chen, Z., Xu, Z., Jiang, A., 2009. Application of immobilized psychrotrophs in ICCBR to treat domestic

Reactors	Parameters	Time (day)							
		0	2	6	9	11	15	22	29
SBR-1	SV_{30} (%)	28	38	32	27	29	26	31	29
	MLSS (mg/L)	4616	3309	3437	4493	4592	4145	4676	4450
	SOUR (mg O_2/(g MLSS·hr))	4.80	2.27	4.94	4.66	4.79	4.36	4.66	4.79
	R-COD_{Cr} (%)	77.60	15.06	88.57	89.64	90.70	91.41	89.26	89.59
SBR-2	SV_{30} (%)	31	44	36	27	31	28	25	34
	MLSS (mg/L)	4634	3447	4260	4311	4338	4473	4290	4122
	SOUR (mg O_2/(g MLSS·hr))	4.67	2.56	4.70	4.26	4.92	4.52	4.34	4.67
	R-COD_{Cr} (%)	75.97	13.14	91.11	87.86	89.42	88.96	92.72	90.54

Table 2 – Characteristics of activated sludge in the SBRs.

SV_{30}: sludge settling ratio; MLSS: Mixed liquor suspended solids; SOUR: Specific oxygen uptake rate; R-CODcr: Removal efficiency of COD.

wastewater and its microbiological investigation. Chin. Sci. Bull. 54 (9), 1599–1606.

Bruning-Fann, C.S., Kaneene, J., 1993. The effects of nitrate, nitrite and N-nitroso compounds on human health: a review. Vet. Hum. Toxicol. 35 (6), 521–538.

CEPB, 2002. Analysis Methods for Water and Wastewater. China Environmental Science Press, Beijing.

Chen, G.H., Yip, W.K., Mo, H.K., Liu, Y., 2001. Effect of sludge fasting/feasting on growth of activated sludge cultures. Water Res. 35 (4), 1029–1037.

Chevalier, P., Proulx, D., Lessard, P., Vincent, W., de la Noue, J., 2000. Nitrogen and phosphorus removal by high latitude mat-forming cyanobacteria for potential use in tertiary wastewater treatment. J. Appl. Phycol. 12 (2), 105–112.

de Kreuk, M., Pronk, M., van Loosdrecht, M., 2005. Formation of aerobic granules and conversion processes in an aerobic granular sludge reactor at moderate and low temperatures. Water Res. 39 (18), 4476–4484.

Dong, Y., Zhang, Z., Jin, Y., Li, Z., Lu, J., 2011. Nitrification performance of nitrifying bacteria immobilized in waterborne polyurethane at low ammonia nitrogen concentrations. J. Environ. Sci. 23 (3), 366–371.

Dong, Y., Zhang, Z., Jin, Y., Lu, J., Cheng, X., Li, J., Deng, Y.Y., Feng, Y.N., Chen, D., 2012. Nitrification characteristics of nitrobacteria immobilized in waterborne Polyurethane in wastewater of corn-based ethanol fuel production. J. Environ. Sci. 24 (6), 999–1005.

Eshchar, M., Lahav, O., Mozes, N., Peduel, A., Ron, B., 2006. Intensive fish culture at high ammonium and low pH. Aquaculture 255 (1), 301–313.

Fdz-Polanco, F., Villaverde, S., Garcia, P., 1994. Temperature effect on nitrifying bacteria activity in biofilters: activation and free ammonia inhibition. Water Sci. Technol. 30 (11), 121–130.

Fitzgerald, C.M., Camejo, P., Oshlag, J.Z., Noguera, D.R., 2015. Ammonia-oxidizing microbial communities in reactors with efficient nitrification at low-dissolved oxygen. Water Res. 70 (1), 38–51.

Gikas, P., Livingston, A., 1998. Use of specific ATP concentration and specific oxygen uptake rate to determine parameters of a structured model of biomass growth. Enzym. Microb. Technol. 22 (6), 500–510.

Gomez-Alvarez, V., Schrantz, K.A., Pressman, J.G., Speitel Jr., G.E., Wahman, D.G., 2013. Pyrosequencing analysis of bench-scale nitrifying biofilters removing trihalomethanes. Environ. Eng. Sci. 30 (9), 582–588.

Hashimoto, N., Sumino, T., 1998. Wastewater treatment using activated sludge entrapped in polyethylene glycol prepolymer. J. Ferment. Bioeng. 86 (4), 424–426.

Hou, J., Miao, L., Wang, C., Wang, P., Ao, Y., Qian, J., et al., 2014. Inhibitory effects of ZnO nanoparticles on aerobic wastewater biofilms from oxygen concentration profiles determined by microelectrodes. J. Hazard. Mater. 276, 164–170.

Huang, Z., Qie, Y., Wang, Z., Zhang, Y., Zhou, W., 2015. Application of deep-sea psychrotolerant bacteria in wastewater treatment by aerobic dynamic membrane bioreactors at low temperature. J. Membr. Sci. 475 (1), 47–56.

Isaka, K., Yoshie, S., Sumino, T., Inamori, Y., Tsuneda, S., 2007. Nitrification of landfill leachate using immobilized nitrifying bacteria at low temperatures. Biochem. Eng. J. 37 (1), 49–55.

Isaka, K., Date, Y., Kimura, Y., Sumino, T., Tsuneda, S., 2008. Nitrogen removal performance using anaerobic ammonium oxidation at low temperatures. FEMS Microbiol. Lett. 282 (1), 32–38.

Isaka, K., Kimura, Y., Osaka, T., Tsuneda, S., 2012. High-rate denitrification using polyethylene glycol gel carriers entrapping heterotrophic denitrifying bacteria. Water Res. 46 (16), 4941–4948.

Khardenavis, A.A., Kapley, A., Purohit, H.J., 2007. Simultaneous nitrification and denitrification by diverse Diaphorobacter sp. Appl. Microbiol. Biotechnol. 77 (2), 403–409.

McKenna, P., Hoffmann, C., Minkah, N., Aye, P.P., Lackner, A., Liu, Z., et al., 2008. The macaque gut microbiome in health, lentiviral infection, and chronic enterocolitis. Plos Pathog. 4 (2), e20.

Qiao, X.L., Liu, Z., Liu, Z.W., Zeng, Y.L., Zhang, Z.J., 2010. Immobilization of activated sludge in poly (ethylene glycol) by UV technology and its application in micro-polluted wastewater. Biochem. Eng. J. 50 (1-2), 71–76.

Salem, S., Berends, D., Heijnen, J., Van Loosdrecht, M., 2003. Bio-augmentation by nitrification with return sludge. Water Res. 37 (8), 1794–1804.

Sudarno, U., Winter, J., Gallert, C., 2011. Effect of varying salinity, temperature, ammonia and nitrous acid concentrations on nitrification of saline wastewater in fixed-bed reactors. Bioresour. Technol. 102 (10), 5665–5673.

Sumino, T., Nakamura, H., Mori, N., Kawaguchi, Y., 1992. Immobilization of nitrifying bacteria by polyethylene glycol prepolymer. J. Ferment. Bioeng. 73 (1), 37–42.

Ward, M.H., DeKok, T.M., Levallois, P., Brender, J., Gulis, G., Nolan, B.T., et al., 2005. Workgroup report: drinking-water nitrate and health—recent findings and research needs. Environ. Health Perspect. 113 (11), 1607–1614.

Weon, H.Y., Yoo, S.H., Kim, Y.J., Lee, C.M., Kim, B.Y., Jeon, Y.A., et al., 2009. Rudaea cellulosilytica gen. nov., sp. nov., isolated from soil. Int. J. Syst. Evol. Microbiol. 59 (9), 2308–2312.

Wu, C., Chen, Z., Liu, X., Peng, Y., 2007. Nitrification–denitrification via nitrite in SBR using real-time control strategy when treating domestic wastewater. Biochem. Eng. J. 36 (2), 87–92.

Xiao, Y., Wu, S., Yang, Z., Wang, Z., Yan, C., Zhao, F., 2013. In situ probing the effect of potentials on the microenvironment of heterotrophic denitrification biofilm with microelectrodes. Chemosphere 93 (7), 1295–1300.

Zhang, X., Yue, S., Zhong, H., Hua, W., Chen, R., Cao, Y., et al., 2011. A diverse bacterial community in an anoxic quinoline-degrading bioreactor determined by using pyrosequencing and clone library analysis. Appl. Microbiol. Biotechnol. 91 (2), 425–434.

Zhong, F., Wu, J., Dai, Y., Yang, L., Zhang, Z., Cheng, S., et al., 2014. Bacterial community analysis by PCR-DGGE and 454-pyrosequencing of horizontal subsurface flow constructed wetlands with front aeration. Appl. Microbiol. Biotechnol. 99 (3), 1–14.